Application of NMR Microimaging by Radio-Frequency Field Gradients to the Observation of Solvent Penetration in Polymeric Materials

P. Maffei,† L. Kiéné,‡ and D. Canet*,†

Groupe de Méthodologie RMN (U.R.A. CNRS No. 406 (LESOC)), Université de Nancy I, B.P. 239, 54506 Vandœuvre lès Nancy Cedex, France, and CIRSEE (Lyonnaise des Eaux-Dumez), 38, rue du président Wilson, 78230 Le Pecq, France

Received May 20, 1992; Revised Manuscript Received July 30, 1992

ABSTRACT: A recently developed NMR microscopy technique based on radio-frequency field gradients is employed to study the penetration of toluene in poly(vinyl chloride), of acetic acid in cellulose, and of *n*-pentane in polystyrene. In spite of broad NMR lines in the two latter cases, good-quality images are still obtained. This is made possible by the inherent features of the proposed imaging technique, which does not need any spin echo or gradient echo and therefore does not suffer from the strong attenuation due to short transverse relaxation times.

Introduction

Several studies of solvent diffusion in polymers by NMR imaging have appeared in the last few years.[1-9] The technique is nondestructive and noninvasive; it allows one therefore to monitor the diffusion process and, in principle, to quantify the solvent concentration at a given location inside the material. Conventional NMR imaging methods[10] rely on the use of static field gradients (B_0 gradients) and generally involve spin echoes or gradient echoes for refocusing nuclear magnetization and/or avoiding artifacts due to gradient switching. Any echo entails, however, some magnetization loss (thus, at the outset, some sensitivity loss) because of transverse relaxation. The latter process is characterized by the transverse relaxation time T_2, or, equivalently, by the line width at half-height of the NMR line, $\Delta\nu = 1/(\pi T_2)$. We make here a distinction between the *natural line width*, which is solely governed by the transverse relaxation time T_2, and the *effective line width*, governed by T_2^*, which includes effects of static field inhomogeneities. These latter effects can be accommodated by spin-echo techniques in conventional NMR imaging, and we shall focus here on consequences of short *natural* T_2. Depending on the natural line width of the solvent NMR line, the sensitivity loss is more or less severe but may become unacceptable when solvent molecules are tightly bound to the polymer, resulting in quite short T_2. Moreover, it is well known that spatial resolution in NMR imaging by B_0 gradients is ultimately dictated by possible magnetic susceptibility variations across the sample[11,12] and/or by diffusion effects.[13,14]

The method employed here makes use of radio-frequency (rf) field gradients (B_1 gradients) without the necessity to have recourse to spin echoes. Furthermore, it is based on *nutation* around the B_1 radio-frequency field, and not on *precession* with respect to the static field B_0 as in conventional NMR imaging techniques. As a consequence, the method is not subjected to the shortcomings associated with nuclear precession. These include effects of (i) variation of magnetic susceptibility and, because no echo is needed, (ii) rapid transverse relaxation and (iii) translational diffusion.

Some examples, relevant to soaked polymers, will be presented to illustrate these features. The first example, toluene in poly(vinyl chloride), is just shown to demonstrate that, provided NMR line widths are those of a normal liquid, images by B_1 gradients are of quality comparable to those obtained by conventional techniques on similar systems. Conversely, the next two examples (acetic acid in cellulose and *n*-pentane in polystyrene) demonstrate the pontentiality of the present method when dealing with systems possessing inherent short transverse relaxation times.

NMR Microimaging by B_1 Gradients

The very first incitement to develop a NMR imaging method based solely on rf gradients is to free oneself from the ill effects due to the switching of static field gradients. These include eddy currents created in materials surrounding the probe but also spectrometer perturbations due to finite rise and fall times of B_0 gradients. With the hope to circumvent the above-mentioned drawbacks, Hoult[15] first proposed an alternative way to perform the spatial-frequency encoding relying on the application of radio-frequency gradients. This idea led to the so-called "rotating-frame zeugmatography" technique[16] which, however, combined static and radio-frequency fields. We recently proposed a 2D rotating-frame imaging method which leads to good-quality images (spatial resolution of 50 μm or better), based on the exclusive use of rf gradients. The main advantages of this method concern negligibly short gradient switching times and the absence of any distortion due to the interactions which develop in the transverse plane, i.e., perpendicularly to the quantification axis (the B_0 direction). These would include scalar and dipolar interactions as well as isotropic or anisotropic chemical shift effects, as long as the B_1 gradient is applied throughout; this is not exactly the case because acquisition windows, during which the gradient is switched off, have to be allowed in the course of the imaging process (see below). The experimental procedures were described in detail in more specific publications,[17,18] and their essential features will just be recalled here.

The NMR probe is of conventional design (saddle-shaped rf coil for signal detection and production of normal rf pulses) with an additional single-turn coil, tuned at the measuring frequency, which delivers a linear rf gradient across the object under investigation, that is, a B_1 field whose amplitude varies linearly along the direction of the coil axis. Both coils are arranged perpendicularly to minimize leakage and coupling effects (Figure 1). The

* To whom correspondence should be addressed.
† Université de Nancy I.
‡ CIRSEE.

0024-9297/92/2225-7114$03.00/0

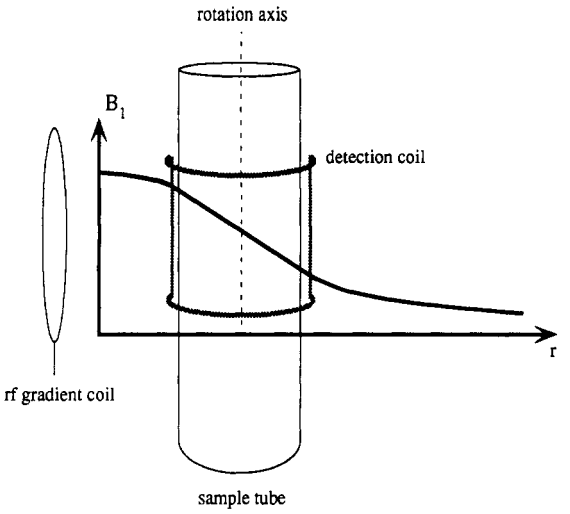

Figure 1. Schematic representation of the NMR probe, together with the profile of the B_1 field created by the rf gradient coil.

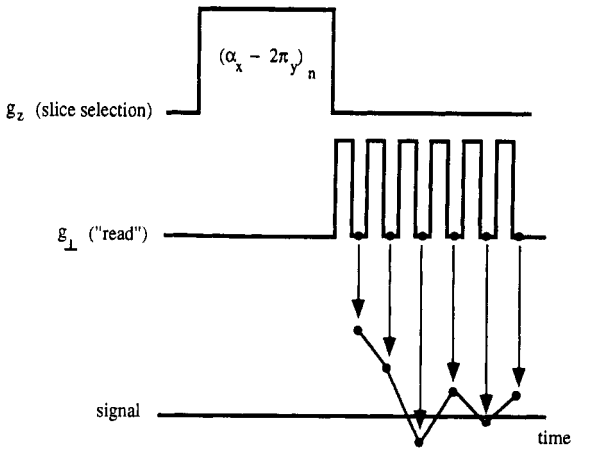

Figure 2. Pulse sequence used for obtaining a one-dimensional image. The rf gradient g_z originates from the saddle-shaped coil. α and 2π refer to flip angles whereas x and y are rf phases. The pulse train is such that $n\alpha = \pi/2$ at the center of the coil. The read gradient $g_\perp$ (created by the "rf gradient coil" of Figure 1) is applied in the form of pulses between which acquisition of the NMR signal takes place.

experiment is based on the Fourier zeugmatography image reconstruction algorithm and is carried out in the following way: first the B_1 gradient is applied for an incremented time interval t_1, producing a (rotating-frame) nutation of nuclear magnetization whose angle depends on the location of the revelant molecules along the axis of the gradient coil, say the X direction. The sample (or the probe) is then rotated by an angle of exactly 90°. This rotation, accomplished in practice by a pneumatic device, takes some time (typically 400 ms), so that all transverse magnetization can be considered to have disappeared whereas the stored longitudinal magnetization is then nutated according to a read B_1 gradient along the Y direction during a time t_2. The double-modulated signal $S(t_1,t_2)$ acquired at the end of this particular 2D NMR experiment directly provides the spatial spin density distribution by means of a double Fourier transformation applied to both variables t_1 and t_2. Two practical points must be mentioned: (i) During the 90° rotation of the sample, longitudinal relaxation manifests itself; this unwanted magnetization recovery is removed by inserting a homogeneous π pulse every other scan together with an acquisition sign alternation. (ii) The NMR receiver cannot be set on during the read gradient application because of residual leakage between the two coils (Figure 2). The gradient is therefore applied in the form of pulses whose duration defines the effective dwell time in the t_2 dimension, the receiver being gated on during acquisition intervals between pulses. A further improvement of image quality arises from a slice selection along the Z direction (the one of the B_0 static field). This is made possible by the strong variation, along that direction, of the B_1 field generated by a purposely designed saddle-shaped coil. As described in a previous publication,[18] the application of a spatial version of a DANTE pulse train permits one to select a slice located at the center of the coil (first part of the scheme shown in Figure 2). This first approach was used for obtaining the images of the two former systems (poly(vinyl chloride) and cellulose) whereas an alternative procedure, now in routine use,[19] was used for the latter system (polystyrene). It consists in obtaining a series of one-dimensional images (profiles) by rotating the object in a stepped manner around the direction of the B_0 axis, thus perpendicular to the B_1 gradient axis. Although both methods carry, in principle, the same amount of information, the latter is favored because it does not entail any sensitivity loss due to the 90° rotation of the sample within the sequence (as in the first method) and because it requires much shorter measuring times. The major difference lies in data treatment which, for the second method, is performed by the so-called filtered-back-projection algorithm,[20] which is especially well suited since the series of profiles represent in fact a series of projections, each of them corresponding to a particular orientation of the object with respect to the gradient.

It can be mentioned that the rf gradient does not pass through zero (Figure 1). This is a decisive advantage since possible offset effects are avoided in the sense that evolution (nutation) is always carried out with a strong B_1. However, a spatial shift occurs and the distance between the rotation axis and the gradient origin has to be injected in the data treatment pertaining to the second method. This distance is simply evaluated by comparing two profiles whose orientations differ exactly by 180°.

Experiments were carried out with a modified WP 200 Bruker spectrometer equipped with a vertical wide-bore magnet and interfaced to a Nicolet 1180 computer. The probe is homemade and the object rotation is performed with apropriate devices: a pneumatic device for the 90° rotation of the first approach, and a stepping motor for the second method. Two rf transmitters are necessary[21] with an adjustable phase relationship. Data are remotely treated on workstations with homemade software, dedicated to the exploitation of this type of experiment.

Permeation of Toluene in Poly(vinyl chloride)

In a first stage, and for concentration evaluation purposes, small rods of poly(vinyl chloride), approximately cylindrically shaped, were cut from pipes supplied by the manufacturer. Their outer diameter is ca. 2.5 mm and their height ca. 50 mm. A rod was immersed in toluene for 15 h and then removed from the solvent and imaged. It was again immersed in toluene for another 15 h, again imaged, and so on. The main reason for which samples were removed from the solvent is the following: because of its large concentration and its long T_2 (transverse relaxation time), the signal from bulk solvent is expected to partially mask the signal from solvent inside the polymer, thus preventing accurate determination of the concentration. On the other hand, a reliable study of the diffusion front advance as well as of the penetration velocity necessitates the sample to be continuously in contact with the solvent to avoid any interruption of the

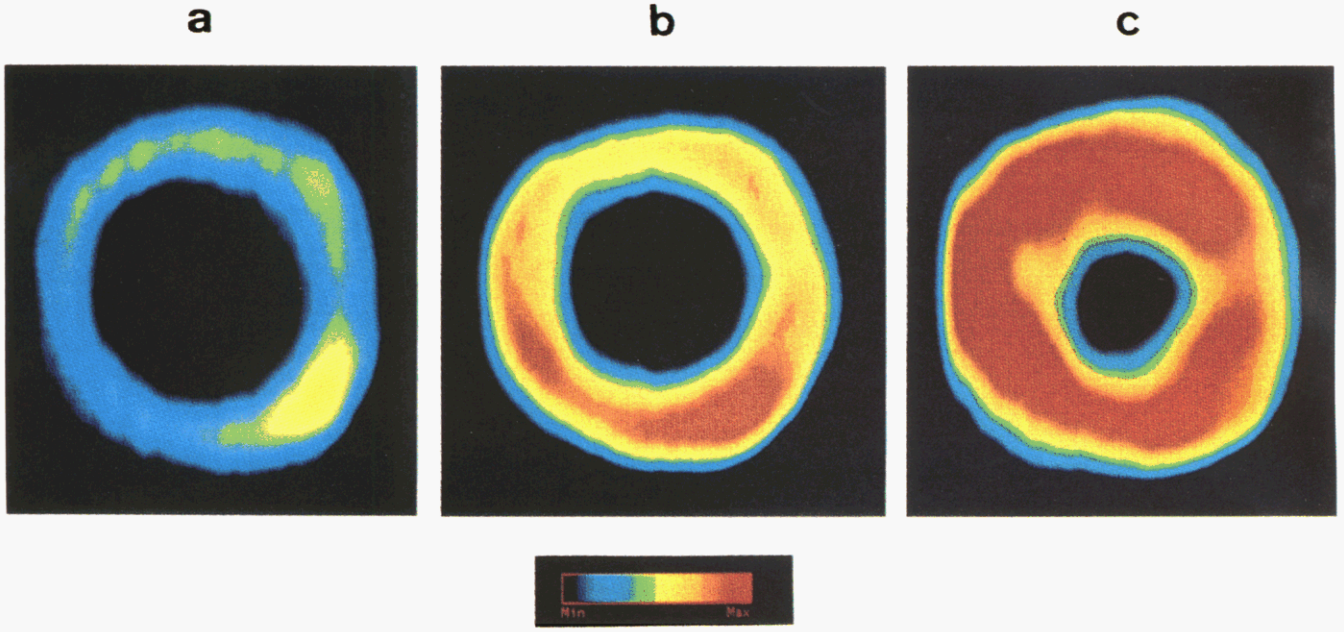

Figure 3. Images showing three stages of the toluene permeation process and the solvent distribution inside poly(vinyl chloride) after (a) 15, (b) 30, and (c) 45 h of exposure. Samples were removed from the solvent prior to the imaging experiment.

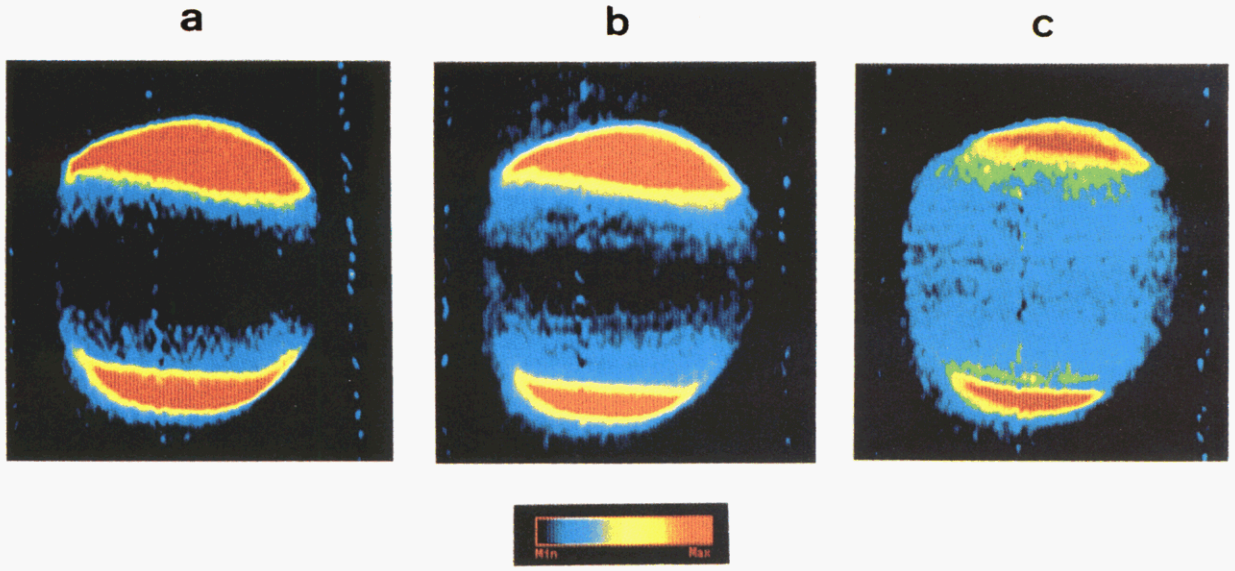

Figure 4. Images showing three steps of the toluene front advance inside poly(vinyl chloride) after (a) 10, (b) 20, and (c) 50 h. Samples were continuously in contact with bulk solvent (red region).

process. For those latter purposes, an additional series of measurements were carried out, according to the following procedure: rectangularly shaped rods of ca. 2 × 3 mm were blocked in 5-mm-o.d. NMR standard tubes filled with toluene, in such a way that only two facets of the PVC sample were actually in contact with the solvent; images were periodically taken without removing the polymer rod from the sample tube. Both series of experiments were carried out at ambient temperature.

Raw data were acquired with 128 and 256 points in both t_1 and t_2 dimensions, respectively, which were extended to a 512 × 512 map by means of zero-filling operations. As we were dealing with rather low-intensity NMR signals, a satisfactory signal-to-noise ratio required 32 accumulated scans for each of the 128 measurements. With a recycle time of 1.5 s between two consecutive scans, the total duration of a typical imaging experiment was about 2 h.

The first series of measurements, detailed above, led to images displayed in Figure 3, corresponding to (a) 15, (b) 30, and (c) 45 h of exposure to toluene, respectively; the color scale, which is also shown on the figure, permits the visualization of the solvent distribution inside the polymeric material. It must be emphasized that these results are presented on an absolute intensity scale, since all experiments have been performed under identical conditions. This implies that the color level corresponding to the highest NMR signal concerns the highest local concentration. In all these images, the outer edge of the sample appears with a lower solvent concentration level. This is presumably due to a desorption process, which takes place during the imaging experiment, and entails some inaccuracy in the concentration calculation. Moreover, it is interesting to observe that some regions are filled faster than others; we suppose that this fact is related with fabrication flaws. The second series of experiments produces the images of Figure 4, in which the front advance can be visualized after (a) 10, (b) 20, and (c) 50 h of exposure to toluene, respectively. It is recalled that during these imaging experiments the polymer was not removed from the tube containing the solvent, so that red color corre-

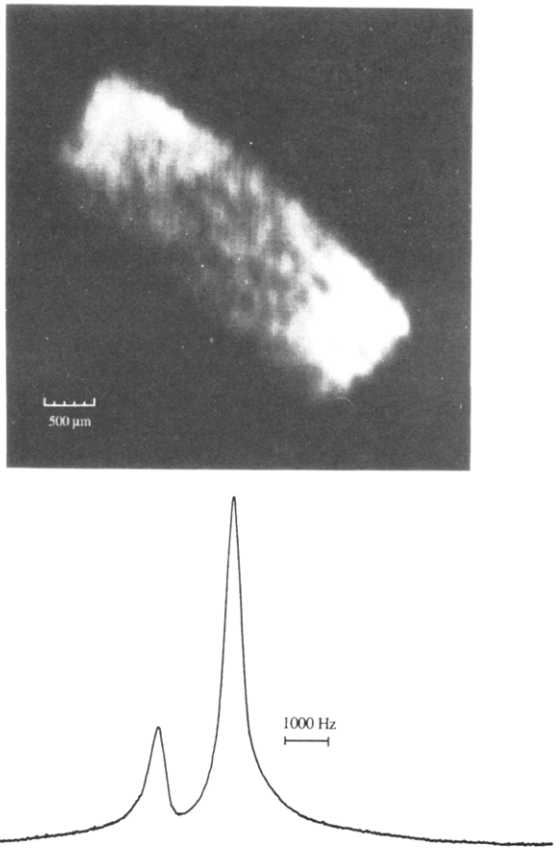

Figure 5. Top: image of a cellulose sample after 48 h of exposure to acetic acid vapors (measuring time: ca. 8 h). Bottom: the corresponding proton NMR spectrum.

sponds to bulk toluene whereas the green and blue regions correspond to imbibed polymer (the bulk solvent area becomes smaller as the polymer swells, filling nearly all the space inside the NMR tube). In this case, because of the shape of the sample (see above), a nearly rectilinear front advance is expected and is indeed observed, as can be seen on the relevant images. Its position as a function of time was calculated by direct measurement on images and suggests that the penetration process occurs according to a constant velocity whose average value was found to be 4.8 nm s^{-1}. Finally, it can be noticed that images displayed on Figure 4 have a lower signal-to-noise ratio than those shown on Figure 3. This is due to a purposely reduced measuring time in the second series of experiments, in order to minimize diffusion effects during the imaging process.

Cellulose Imbibed with Acetic Acid

Cellulose is probably one of the most important natural polymers used for industrial applications. Among these applications, the production of cellulose acetate is of some interest. A first step in the whole process concerns the replacement of water tightly bound to cellulose by acetic acid. In this context, it may appear interesting to get some insight into the reactant penetration in such a material by NMR microimaging. However, acetic acid may also tightly bind to cellulose and, depending on its concentration, lead to more or less broad NMR lines which are not very adequate for imaging purposes. This broadening originates from restricted mobility or sample inhomogeneity. The purpose of the present example is to demonstrate the feasibility of NMR microimaging by rf gradients with an acceptable spatial resolution in spite of broadened NMR lines.

Samples were small enough for obtaining detailed information (on a scale smaller than 100 μm) about (i) the homogeneity of the reactant distribution within the sample and (ii) the preferred penetration as a function of the local surface state of cellulose. To examine the acetic acid actually interacting with the polymer, cellulose was not immersed but rather subjected to saturating vapors of the reactant for ca. 48 h. At the end of this process, a small piece of ca. 4-mm width was cut and inserted in a regular 5-mm NMR tube in such a way that the cellulose sample was held against the tube wall. A conventional NMR spectrum was recorded for control purposes. It is shown at the bottom of Figure 5. Both resonances (CH_3 and OH) exhibit line widths of the order of 300 Hz. This

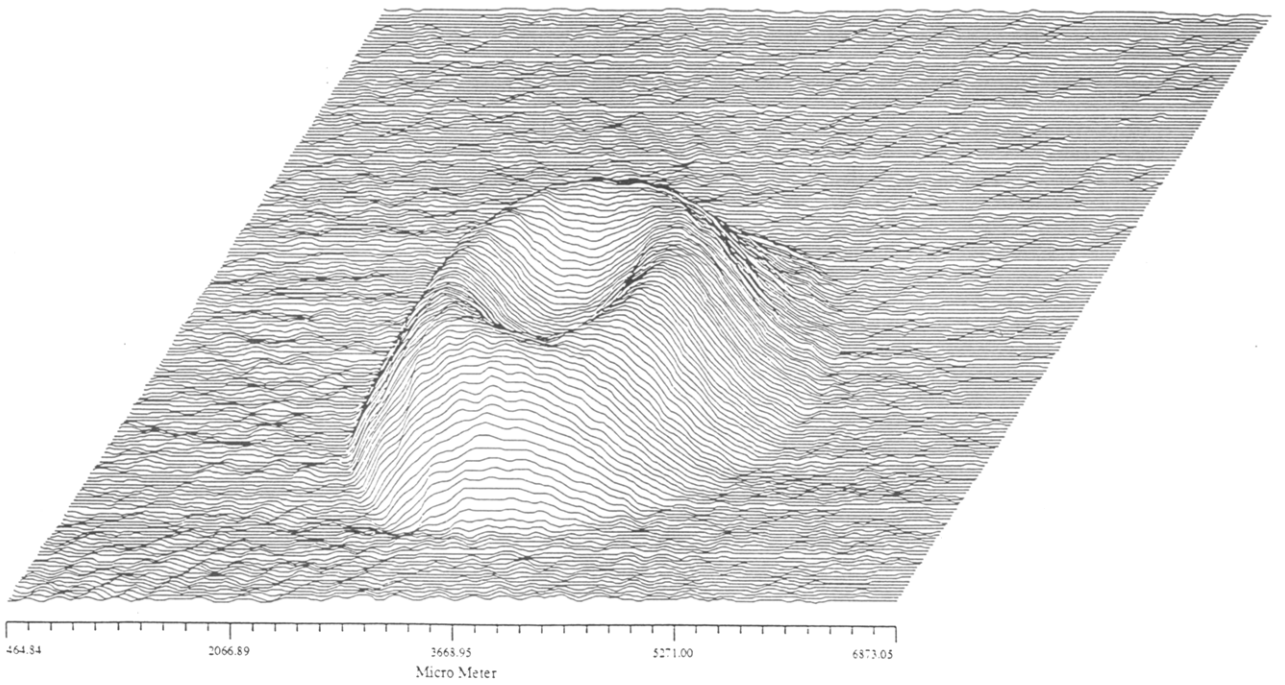

Figure 6. Traces whose amplitudes indicate the spatial concentration of *n*-pentane inside a rod of polystyrene (measuring time: ca. 6 h).

broadening may have two origins: (i) a T_2 shortening arising from a reduced mobility of acetic acid which is, for its major part, bound to the polymer (this arises from the mode according to which the sample has been prepared) and (ii) the inhomogeneous nature of the sample itself. Conversely, longitudinal relaxation times T_1 have usual values (around 1 s, as can be estimated from the waiting time (4 s) that has to be used in imaging experiments). This difference in transverse and longitudinal relaxation times can be explained as follows: T_2 is partly affected by the slow motion of the polymer, through a spectral density at zero frequency which becomes predominant, whereas T_1, which depends solely on spectral densities at the measurement frequency and twice this measurement frequency, is only sensitive to fast motions, which are very likely to occur as local rotations and to be efficient even for bound molecules.

Figure 5 (top) is an image showing the distribution of acetic acid within that cellulose sample. The fact that we observe details whose dimensions may be as low as 100 μm demonstrates the spatial resolution which can be obtained. The intrinsic spatial resolution of the method, which would be better appreciated with long T_2 systems, will be discussed elsewhere.[19] For the moment, let us express this quantity as a function of the line width by $\Delta x = \Delta\nu/\gamma g_1$, where γ is the gyromagnetic ratio of proton and g_1 the applied gradient. This yields here, with g_1 lying around 2 G cm^{-1}, a value of $\Delta\nu$ which must not exceed 700 Hz for reaching such a spatial resolution (100 μm). As far as the present example is concerned, we are far beyond the upper limit mentioned above, which will, however, fully apply in the next example. The acetic acid distribution inside the sample is far from being uniform: there is a significant loss at the center. This observation can be interpreted in the following way: the sheet of cellulose was cut at the dimension of the NMR tube before being exposed to acetic acid vapors. This corresponds to the two sides of the images whereas the largest dimension corresponds to the smooth surfaces of the cellulose sheet. It can therefore be concluded that acetic acid preferentially penetrates in the cellulose material through a rough surface (the sides of which have been cut).

n-Pentane in Polystyrene

This last example concerns a more difficult situation which involves NMR line widths of the order of 800 Hz. This case deals with *n*-pentane inside a rod of polystyrene of approximately 2-mm diameter. It is known that expansion of the polymer can be mediated by the presence of *n*-pentane, and it may be important to determine the solvent distribution inside the polymeric material, possibly as a function of the time elapsed since the initial contact of polystyrene with *n*-pentane. Obtaining a NMR image of such a sample is made difficult by (i) the relatively small amount of solvent present in the polymer and (ii) more problematic, the important line width of *n*-pentane which arises from its strong interaction with the polymer, a situation already met in the case of acetic acid and cellulose. Nevertheless, the use of B_1 gradients does allow us to obtain this quantitative information, as shown in the stacked plot of Figure 6. This presentation is more informative than the image itself (not shown) since the local concentration can be directly measured by the amplitude of each trace. For this particular sample, examined 3 days after impregnation of a polystyrene rod in *n*-pentane, which resulted in 11% in weight of solvent in the polymer, it can be seen that the core is little impregnated. A complete quantitative study is in progress and will be presented elsewhere.

Conclusion

It must be emphasized that the line width mentioned in the above example corresponds to an effective transverse relaxation time of 400 μs, which could hardly be accommodated by procedures based on spin echoes or gradient echoes. As far as the standard method of imaging by B_0 gradients is used, the interval allowed for echo refocusing is generally of the order of a few milliseconds; during this interval, T_2 processes are fully operative and, in such a case, would make difficult the formation of any image. Fortunately, methodologies presented here do not require any echo prior to data acquisition and are therefore adequate for imaging solvents strongly interacting with the polymer. On the other hand, as demonstrated by the first example, the method yields results comparable to conventional imaging when dealing with sharp NMR signals. Moreover, its easy implementation on a conventional NMR spectrometer should make it widely applicable in the field of material science. In this respect, further developments, which rely on improvements of probe design, should be directed to the reduction of the measuring time and to a better spatial resolution by decreasing the interval allotted to signal acquisition.

Acknowledgment. We are grateful to a referee whose comments led to the improvement of the manuscript. It is a pleasure to thank K. Elbayed for his experimental help and Dr. P. Lancelin (Rhône-Poulenc), Dr. L. Trognon, and Dr. R.-P. Eustache (Atochem) for their cooperation. We gratefully acknowledge financial support from Lyonnaise des Eaux-Dumez (Le Pecq), Rhône-Poulenc (Décines), and Atochem (Serquigny).

References and Notes

(1) Koenig, J. L. *Appl. Spectrosc.* **1989**, *43*, 1117.
(2) Weisenberger, L. A.; Koenig, J. L. *Macromolecules* **1990**, *23*, 2445.
(3) Weisenberger, L. A.; Koenig, J. L. *Macromolecules* **1990**, *23*, 2454.
(4) Smith, S. R.; Koenig, J. L. *Macromolecules* **1991**, *24*, 3496.
(5) Grinsted, R. A.; Koenig, J. L. *Macromolecules* **1992**, *25*, 1229.
(6) Grinsted, R. A.; Clark, L.; Koenig, J. L. *Macromolecules* **1992**, *25*, 1235.
(7) Rothwell, W. P.; Gentempo, P. P. *Bruker Rep.* **1985**, *1*, 46.
(8) Chang, C.; Komoroski, R. A. *Macromolecules* **1989**, *22*, 600.
(9) Blümich, B.; Blumler, P.; Gunther, E.; Schauss, G. *Bruker Rep.* **1990**, *2*, 22.
(10) See, for instance: Osment, K. A.; Packer, K. J.; Taylor, M. J.; Attard, J. J.; Carpenter, T. A.; Hall, L. D.; Herrod, N. J.; Dorand, S. J. *Philos. Trans. R. Soc. London* **1990**, *333*, 441.
(11) Callaghan, P. T. *J. Magn. Reson.* **1990**, *87*, 304.
(12) Bowtell, R. W.; Brown, G. D.; Glover, P. M.; McJury, M.; Mansfield, P. *Philos. Trans. Soc. London* **1990**, *333*, 457.
(13) Callaghan, P. T.; Eccles, C. D. *J. Magn. Reson.* **1988**, *78*, 1.
(14) Hyslop, W. B.; Lauterbur, P. C. *J. Magn. Reson.* **1991**, *94*, 501.
(15) Hoult, D. I. *J. Magn. Reson.* **1984**, *33*, 183.
(16) Chen, C. N.; Hoult, D. I.; Sank, V. J. *Mag. Reson. Med.* **1984**, *1*, 354.
(17) Boudot, D.; Montigny, F.; Elbayed, K.; Mutzenhardt, P.; Diter, B.; Brondeau, J.; Canet, D. *J. Magn. Reson.* **1991**, *92*, 605.
(18) Maffei, P.; Elbayed, K.; Brondeau, J.; Canet, D. *J. Magn. Reson.* **1991**, *95*, 382.
(19) Maffei, P.; Mutzenhardt, P.; Retournard, A.; Brondeau, J.; Canet, D., to be published.
(20) Callaghan, P. T. *Principles of NMR Microscopy*; Clarendon: Oxford, 1991.
(21) Canet, D.; Diter, B.; Belmajdoub, A.; Brondeau, J.; Boubel, J.-C.; Elbayed, K. *J. Magn. Reson.* **1989**, *81*, 1.

Registry No. PVC, 9002-86-2; AA, 64-19-7; PS, 9003-53-6; toluene, 108-88-3; cellulose, 9004-34-6; *n*-pentane, 109-66-0.